On the occurrence of fast neutrino flavor conversions in multidimensional supernova models

Sajad Abbar,[1,2] Huaiyu Duan,[2] Kohsuke Sumiyoshi,[3] Tomoya Takiwaki,[4] and Maria Cristina Volpe[1]

[1]*Astro-Particule et Cosmologie (APC), CNRS UMR 7164, Université Denis Diderot, 75205 Paris Cedex 13, France*

[2]*Department of Physics & Astronomy, University of New Mexico, Albuquerque, New Mexico 87131, USA*

[3]*Numazu College of Technology, Ooka 3600, Numazu, Shizuoka 410-8501, Japan*

[4]*National Astronomical Observatory of Japan, Osawa, Mitaka, Tokyo 181-8588, Japan*

(Received 17 December 2018; published 7 August 2019)

The dense neutrino medium in a core-collapse supernova or a neutron-star merger event can experience fast flavor conversions on time/distance scales that are much smaller than those of vacuum oscillations. It is believed that fast neutrino flavor transformation occurs in the region where the angular distributions of ν_e and $\bar{\nu}_e$ cross each other. We present the first study of this crossing phenomenon and the fast neutrino flavor conversions in multidimensional (multi-D) supernova models. We examine the neutrino distributions obtained by solving the Boltzmann transport equation for several fixed profiles which are representative snapshots taken from separate 2D and 3D supernova simulations with an 11.2 $M_\odot$ progenitor model. Our research shows that the spherically asymmetric patterns of the ν_e and $\bar{\nu}_e$ fluxes in multi-D models can assist the appearance of the crossing between the ν_e and $\bar{\nu}_e$ angular distributions. In the models that we have studied, there exist unstable neutrino oscillation modes in and beyond the neutrino decoupling region which have amplitude growth rates as large as an e-fold per nanosecond. This finding can have important consequences for the explosion mechanism, nucleosynthesis, and neutrino signals of core-collapse supernovae.

DOI: 10.1103/PhysRevD.100.043004

I. INTRODUCTION

At the exhaustion of its nuclear fuel, the stellar core of a massive star collapses under its own gravity into a neutron star or black hole, and the rest of the star either explodes as a supernova or falls back to become a part of the black hole. In a successful explosion, the hot protoneutron star (PNS) formed at the center of the (core-collapse) supernova quickly cools down by emitting $\sim 10^{58}$ neutrinos in all flavors in just tens of seconds. Although the exact mechanism of the supernova explosion remains elusive, the neutrino reactions

$$\bar{\nu}_e + p \rightleftharpoons n + e^+ \quad \text{and} \quad \nu_e + n \rightleftharpoons p + e^- \qquad (1)$$

are known to be important in the heating and cooling of the matter deep inside the supernova and can play an important role in exploding the star [1–3]. Supernova ejecta are also one of the few places in the universe where the heavy elements can be abundantly produced. An important factor that regulates the nucleosynthesis in the supernova ejecta is its electron fraction Y_e (defined as the ratio of the net number density of the electrons to that of the baryons or n_e/n_b) [4] which in turn is determined by the neutrino processes in Eq. (1). Because these processes involve only ν_e and $\bar{\nu}_e$, and because the neutrinos in different flavors are emitted in different intensities and energies in a supernova, the transformation or oscillations between different neutrino flavors ($\nu_e \rightleftharpoons \nu_{\mu/\tau}$ and $\bar{\nu}_e \rightleftharpoons \bar{\nu}_{\mu/\tau}$) near or even inside the surface of the PNS can have a significant impact on the nucleosynthesis in the supernova ejecta and the supernova dynamics. Understanding the flavor transformation of the neutrinos inside the supernova is also crucial to the prediction of the neutrino signals from future galactic supernovae and the neutrino diffuse background [5–9].

Because of the coherent forward scattering by the dense neutrino medium surrounding the PNS, supernova neutrinos can experience collective flavor transformation [10–14] which occurs much deeper than does the flavor conversion induced by matter alone through the Mikheyev-Smirnov-Wolfenstein (MSW) mechanism [15–17]. However, based on the stationary neutrino bulb model [11] in which all neutrinos are decoupled from matter at a single sharp neutrino sphere, it was found that collective flavor transformation is suppressed during the accretion phase of the supernova due to the large density of the ambient matter [18–21] and/or even the neutrinos themselves [22]. Although, in the more realistic models that evolve with time and does not have the spherical symmetry, this suppression can be lifted for the collective modes that oscillate rapidly in space and time [23–27], the physical conditions can change significantly before these modes have a sufficient growth in amplitudes to engender significant flavor conversions.

In a real supernova, the neutrinos of different flavors (and energies) decouple from matter at different depths of the PNS and have different angular distributions outside the PNS. As a result, fast neutrino flavor conversions can be driven by the neutrino density n_ν which occur on a characteristic length scale $l_{\text{fast}} \sim (\hbar c)^{-2} G_F^{-1} n_\nu^{-1}$ with G_F being the Fermi coupling constant of the weak interaction [28–36]. Such flavor transformation is rightly called fast because l_{fast} is much shorter than the typical wavelength of vacuum oscillations ($\sim\mathcal{O}(1)$ km for a 10 MeV neutrino with the atmospheric neutrino mass splitting) and even the mean free path of the neutrino inside the PNS [37]. It is believed that fast neutrino flavor conversions occur only where the angular distributions of ν_e and $\bar{\nu}_e$ cross each other [31,34]. However, an earlier study of the one-dimensional (1D) supernova models of the Garching group with the Boltzmann neutrino transport did not reveal any scenario with such crossed neutrino angular distributions or fast neutrino flavor conversions [38]. It has been speculated [30,34] that the multi-D models exhibiting the lepton-emission self-sustained asymmetry (LESA) [39] may have regions that foster fast flavor conversions. But the neutrino transports in most of the existing multi-D supernova simulations are implemented with various approximations and do not provide detailed angular distributions of the neutrinos.

Recently, the full information of the neutrino angular distributions became available to multi-D supernova models by directly solving the Boltzmann equation in three momentum dimensions [40]. This approach has been used to study the neutrino transport in supernova cores [41] and its impact on the explosion dynamics [42].

In this paper, we present the first survey of the neutrino angular distributions in multi-D supernova models to ascertain the physical conditions under which fast neutrino flavor conversions may occur.

II. NEUTRINO TRANSPORT AND FAST FLAVOR CONVERSIONS

At each space-time point $(t, \mathbf{r})$, the flavor content of the neutrino medium in the momentum mode $\mathbf{p}$ can be specified by its flavor density matrix $\varrho_{\mathbf{p}}(t, \mathbf{r})$ [43] which, for two flavors (e and x) and in the weak-interaction basis, is [44]

$$\varrho = \frac{f_{\nu_e} + f_{\nu_x}}{2} + \frac{f_{\nu_e} - f_{\nu_x}}{2} \begin{bmatrix} s & S \\ S^* & -s \end{bmatrix}, \tag{2}$$

where f_{ν_e/ν_x} are the initial occupation numbers in the corresponding flavors, and the complex and real scalar fields S and s describe the flavor coherence and the flavor conversion of the neutrino, respectively. A similar expression exists for the flavor density matrix $\bar{\varrho}$ of the antineutrino. The flavor evolution of the neutrino medium is governed by the Liouville-von Neumann equation [43,45–48]

$$i(\partial_t + \mathbf{v}\cdot\nabla)\varrho_{\mathbf{p}} = \left[\frac{\mathsf{M}^2}{2E_\nu} + \frac{\lambda}{2}\sigma_3 + \mathsf{H}_{\nu\nu,\mathbf{p}}, \varrho_{\mathbf{p}}\right] + \mathcal{C}[\varrho_{\mathbf{p}}], \tag{3}$$

where we have adopted the natural units $c = \hbar = 1$. In the above equation, $E_\nu = |\mathbf{p}|$, $\mathbf{v} = \mathbf{p}/E_\nu$, and M^2 are the energy, velocity, and mass-square matrix of the neutrino, respectively, $\lambda = \sqrt{2}G_F n_e$ is the matter potential [15,17], σ_3 is the third Pauli matrix,

$$\mathsf{H}_{\nu\nu,\mathbf{p}} = \sqrt{2}G_F \int \frac{\mathrm{d}^3 p'}{(2\pi)^3}(1 - \mathbf{v}\cdot\mathbf{v}')(\varrho_{\mathbf{p}'} - \bar{\varrho}_{\mathbf{p}'}) \tag{4}$$

is the neutrino potential stemming from the neutrino-neutrino forward scattering [49–51], and $\mathcal{C}[\varrho_{\mathbf{p}}]$ denotes the collision, emission and absorption of the neutrinos.

To study fast neutrino flavor conversions, we ignore the vacuum oscillation Hamiltonian $\mathsf{M}^2/2E_\nu$ so that the flavor transformation of the neutrinos becomes energy independent. We also ignore the collision term $\mathcal{C}[\varrho_{\mathbf{p}}]$ and assume that the physical conditions are homogeneous and stationary for the distance and time scales of interest except for the small but rapidly varying flavor mixing amplitude $S_{\mathbf{v}}(t, \mathbf{r})$. This approximation is valid before significant flavor conversion has occurred so that $|S_{\mathbf{v}}| \ll 1$ and $s \approx 1$. In this scenario, it is useful to define the angular distribution of the electron lepton number (ELN) of the neutrino flux as [31]

$$G_{\mathbf{v}} = \sqrt{2}G_F \int_0^\infty \frac{E_\nu^2 \mathrm{d}E_\nu}{(2\pi)^3}[f_{\nu_e}(\mathbf{p}) - f_{\bar{\nu}_e}(\mathbf{p})], \tag{5}$$

where we have assumed $f_{\nu_x}(\mathbf{p}) = f_{\bar{\nu}_x}(\mathbf{p})$. Keeping only the terms in Eq. (3) of magnitude $\mathcal{O}(|S_{\mathbf{v}}|)$ or larger, one obtains [31,44,52]

$$i(\partial_t + \mathbf{v}\cdot\nabla)S_{\mathbf{v}} = (\epsilon_0 + \mathbf{v}\cdot\boldsymbol{\epsilon})S_{\mathbf{v}} - \int \mathrm{d}\Gamma_{\mathbf{v}'}(1 - \mathbf{v}\cdot\mathbf{v}')G_{\mathbf{v}'}S_{\mathbf{v}'}, \tag{6}$$

where $\mathrm{d}\Gamma_{\mathbf{v}'}$ is the differential solid angle in the direction of $\mathbf{v}'$, $\epsilon_0 = \lambda + \int \mathrm{d}\Gamma_{\mathbf{v}'}G_{\mathbf{v}'}$, and $\boldsymbol{\epsilon} = \int \mathrm{d}\Gamma_{\mathbf{v}'}G_{\mathbf{v}'}\mathbf{v}'$.

Collective flavor transformation is induced by the normal modes in the neutrino medium which, in the linear regime (where $|S_{\mathbf{v}}| \ll 1$), are of the form $S_{\mathbf{v}}(t, \mathbf{r}) = Q_{\mathbf{v}}e^{-i\Omega t + i\mathbf{K}\cdot\mathbf{r}}$, where $Q_{\mathbf{v}}$, Ω and $\mathbf{K}$ are constant with the latter two being also independent of $\mathbf{v}$. The flavor mixing amplitude $S_{\mathbf{v}}$ remains small unless for a real wave vector $\mathbf{K}$ the corresponding frequency has a positive imaginary component, i.e., $\Omega_i = \mathrm{Im}(\Omega) > 0$. In this case the wave amplitude can grow exponentially on the time scale of l_{fast}/c. Such unstable normal modes with fast growing amplitudes can exist when the ELN distribution $G_{\mathbf{v}}$ crosses 0 at some angle(s) [31,34].

III. ELN CROSSINGS IN MULTI-D SUPERNOVA MODELS

We study the angular distributions of the neutrinos which are obtained by solving the Boltzmann transport equation (without any flavor transformation) for several fixed supernova profiles [41]. These profiles were taken from the representative snapshots at $t_{\mathrm{pb}} = 100$, 150 and 200 ms post the core bounce, respectively, of a 2D and a 3D supernova simulations by using the Lattimer and Swesty equation of state [53] with an approximate neutrino transport and with an 11.2 $M_\odot$ progenitor model [54,55]. The spatial resolutions of the Boltzmann calculations are (256,64,1) and (256,64,32) for the 2D and 3D models, respectively, for radius up to 2613 km from the original simulations, where (N_r, N_Θ, N_Φ) are the numbers of spatial zones in the spherical coordinates (r, Θ, Φ). The momentum resolution $(N_{E_\nu}, N_{\theta_\nu}, N_{\phi_\nu})$ of the neutrino flux in each spatial zone is (14,6,12), where θ_ν and ϕ_ν are the zenith and azimuthal angles of the neutrino velocity $\mathbf{v}$ with respect to the radial direction, respectively.

Out of the three snapshots of the 2D model we find regions with ELN crossings within and above the decoupling region in the one at $t_{\mathrm{pb}} = 200$ ms. At this time, the deformed shock has reached over 500 km and is poised to explode the star with the help of a bipolar growth of the hydrodynamic instabilities. Depending on their flavors and energies, neutrinos decouple from matter at radius ∼50–70 km which can be viewed as the "surface" or neutrino sphere of the PNS. In the first two panels of Fig. 1 we show the number densities $n_\nu = \int \frac{d^3p}{(2\pi)^3} f_\nu(\mathbf{p})$ and average flux densities $\mathbf{j}_\nu = \int \frac{d^3p}{(2\pi)^3} f_\nu(\mathbf{p})\mathbf{v}$ in this snapshot for $\nu = \nu_e$ and $\bar\nu_e$, respectively. Both n_ν and $\mathbf{j}_\nu$ are mostly spherically symmetric in this snapshot with $\mathbf{j}_\nu$ generally pointing in the radial direction with some cases of nonradial fluxes. Naively, one may think that ELN crossings may occur below the neutrino sphere where $\mathbf{j}_{\nu_e}$ and $\mathbf{j}_{\bar\nu_e}$ can point in very different directions. This is not the case, however, because $f_\nu(\mathbf{p})$ is highly isotropic in this region, and we find no ELN crossing here.

In our study, ELN crossings usually begin to appear in the region where the neutrinos begin to decouple from matter as shown in the right panels of Fig. 1. Furthermore, we find that, at the radii where ELN crossings do occur, they usually appear in the angular zones with the $\bar\nu_e$-to-ν_e ratio $\alpha = n_{\bar\nu_e}/n_{\nu_e}$ close to 1. The correlation between α and ELN crossings is not really a surprise. In the neutrino decoupling region, $f_\nu(\mathbf{p})$ becomes more and more peaked in the forward direction. Because the PNS is rich in neutrons, $\bar\nu_e$'s decouple from matter at smaller radii than ν_e's do and thus obtain a more forwardly peaked distribution. However, this difference in $f_{\nu_e}(\mathbf{p})$ and $f_{\bar\nu_e}(\mathbf{p})$ is usually not large enough to result in an ELN crossing unless $\bar\nu_e$ has a flux density very close to that of ν_e. This is likely the reason why no ELN crossing was found in a previous study of 1D supernova models [38]. In the 2D model presented in Fig. 1, however, α can vary across angular zones at the same radius which leads to ELN crossings in some regions.

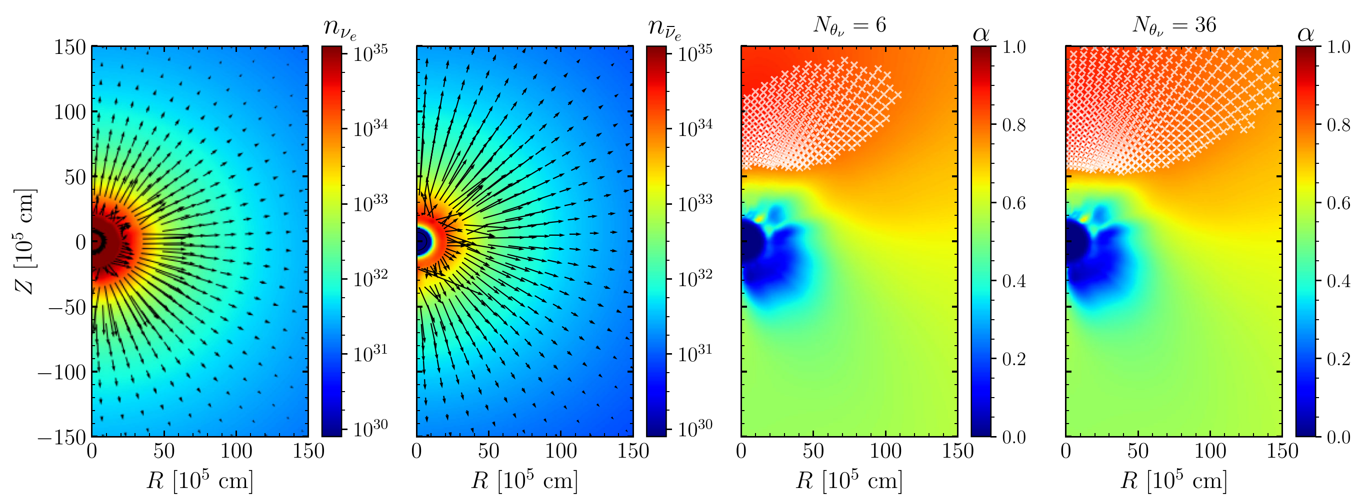

FIG. 1. The neutrino number densities n_{ν_e} and $n_{\bar\nu_e}$ (left panels) and their ratio $\alpha = n_{\bar\nu_e}/n_{\nu_e}$ (right panels) in the $t_{\mathrm{pb}} = 200$ ms snapshot of the 2D supernova model. The lengths and orientations of the arrows in the left panels indicate the magnitudes and directions of the average neutrino flux densities $\mathbf{j}_{\nu_e}$ and $\mathbf{j}_{\bar\nu_e}$ in the corresponding spatial zones. The white crosses in the right panels mark the zones where the ELN crossing occurs. There is almost no difference between angle averaged properties of the neutrinos solved in the low and high resolutions (with $N_{\theta_\nu} = 6$ and 36, respectively) except for the spatial extent over which the ELN crossing occurs.

To check the sensitivity of our results on the angular resolution of the neutrino distributions, we also solve the neutrino transport for the $t_{\mathrm{pb}} = 200$ ms snapshot of the 2D model with $N_{\theta_\nu} = 36$. We find that, although the angle averaged properties of the neutrinos such as n_ν, $\mathbf{j}_\nu$ and α are almost identical for the two calculations, the region with ELN crossings is much wider in the high-resolution calculation than in the one with a lower resolution (right panels of Fig. 1). To find out the reason why some spatial zones show ELN crossings in the high-resolution calculation only, we compare the ELN distributions $G_{\mathbf{v}}$ of these zones in the two calculations. Because $f(\mathbf{p})$ are approximately axially symmetric about the radial direction in our models, we integrated them over ϕ_ν and calculated $f_\nu(\theta_\nu) = \iint \frac{E_\nu^2 \mathrm{d}E_\nu \mathrm{d}\phi_\nu}{(2\pi)^3} f_\nu(\mathbf{p})$ and $G(\theta_\nu) = \int_0^{2\pi} \mathrm{d}\phi_\nu G_{\mathbf{v}}$. We plot $f_{\nu_e}(\theta_\nu)$, $f_{\bar{\nu}_e}(\theta_\nu)$ and $G(\theta_\nu)$ for the spatial zone centered at $r = 65.6$ km and $\cos\Theta = 0.96$ in the first two panels of Fig. 2. From this figure one sees that the coarse angular resolution is sufficient to capture the overall shape of $f_\nu(\theta_\nu)$, and it is more accurate in the backward directions than in the forward directions. However, because the ELN distribution $G(\theta_\nu)$ is sensitive to the small difference between $f_{\nu_e}(\theta_\nu)$ and $f_{\bar{\nu}_e}(\theta_\nu)$, and because it is likely to cross 0 near the radial direction, a high angular resolution in the forward directions is needed to accurately describe the crossing in the neutrino distributions. This issue becomes more severe at large radii where $f_{\nu_e}(\theta_\nu)$ and $f_{\bar{\nu}_e}(\theta_\nu)$ are both highly peaked in the forward direction, and they may cross each other at an angle beyond the last θ_ν bin.

We calculate the exponential growth rates Ω_{i} of the unstable fast oscillation modes as functions of the real wave number K for the (interpolated) ELN distributions plotted in Fig. 2, and the results are shown in the right panel in the same figure. We assume the axial symmetry about the radial direction in calculating Ω_{i}. We also assume that the wave vector of the collective flavor oscillation wave is along the radial direction. In this particular example, $S_{\mathbf{v}}$ can grow by an e-fold within $\sim$1 nanosecond which is indeed much faster than the typical changing rates of the physical conditions inside the supernova.

We also find ELN crossings in the 3D model which seem to be more common than in the 2D model. This observation can be understood by noting that the spatial asymmetries in the neutrino emission might evolve faster in the case of the 3D simulations [56]. They appear in all the three snapshots that we have studied. In the $t_{\mathrm{pb}} = 200$ ms snapshot, ELN crossings begin to occur at $r = 46$ km in the neutrino decoupling region. We show α in this snapshot at $r = 65.6$ km in the left panel of Fig. 3 and mark with crosses the spatial zones where ELN crossings occur. As in the 2D model, ELN crossings are more likely to appear in the regions with α close to 1. The asymmetry pattern in the emissions of ν_e and $\bar{\nu}_e$ is associated with a similar pattern in Y_e which is present even well below the neutrino sphere (middle and right panels of Fig. 3). The region with lower Y_e and more neutron-rich matter emits more $\bar{\nu}_e$'s and absorbs more ν_e's through the reactions in Eq. (1). This pattern of Y_e and α is likely caused by the active matter convection inside the PNS as in the LESA phenomenon [39].

Our study highlights the need of more multi-D supernova simulations with the neutrino Boltzmann transport like those performed in Ref. [42]. Our results show that the neutrino distributions with even a very coarse angular resolution can be used to identify the ELN crossings in the neutrino decoupling region, although a better resolution in the radial direction is needed to accurately describe the crossings especially at large radii. Although we have found fast growing neutrino oscillations in the multi-D models that we have studied, it remains to be seen if the conditions for the ELN crossing will be met in the more self-consistent multi-D supernova simulations with accurate neutrino transport, and if the amplitudes of the fast neutrino oscillation

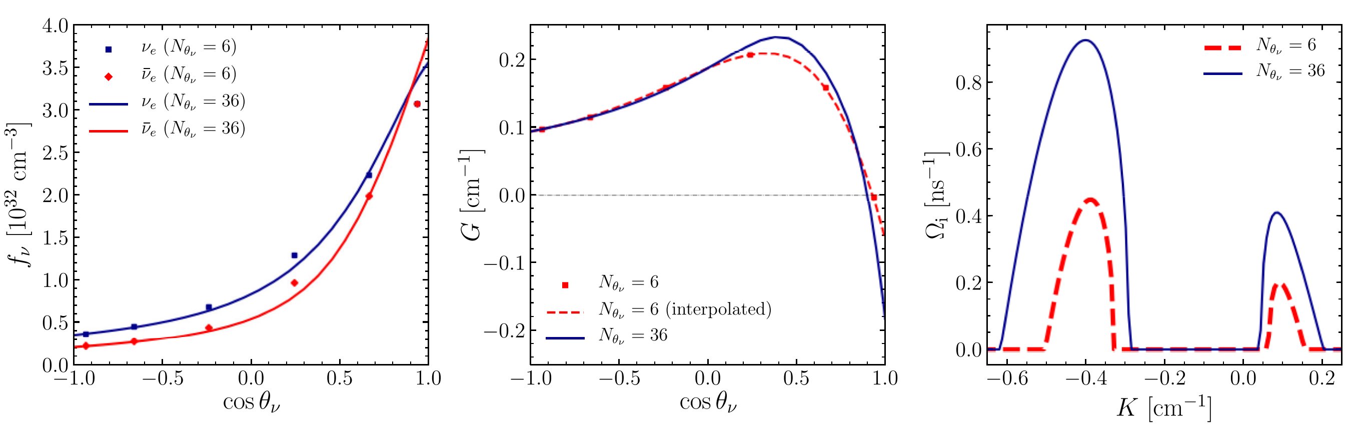

FIG. 2. The neutrino angular distributions $f_{\nu_e}(\theta_\nu)$ and $f_{\bar{\nu}_e}(\theta_\nu)$ (left) and the ELN distribution $G(\theta_\nu)$ (middle) solved in two angular resolutions, $N_{\theta_\nu} = 6$ and 36, respectively, and the corresponding exponential growth rates Ω_{i} as functions of the real wave number K of the fast neutrino oscillation modes propagating in the radial direction. The results are for the spatial zone centered at $r = 65.6$ km and $\cos\Theta = 0.96$ in the 2D model shown in Fig. 1.

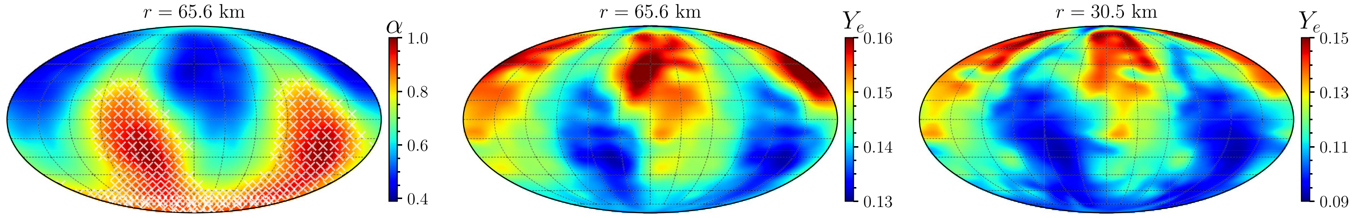

FIG. 3. The Mollweide projection of the $\bar{\nu}_e$-to-ν_e density ratio α at $r = 65.6$ km (left) and the electron fractions Y_e at $r = 65.6$ km and 30.5 km (middle and right), respectively, in the $t_{\mathrm{pb}} = 200$ ms snapshot of the 3D supernova model. The white crosses in the left panel mark the spatial zones where ELN crossings occur.

modes can continue to grow into the nonlinear regime and cause significant flavor conversions deep inside the supernova. If fast neutrino flavor conversions are indeed found to occur near the surface of the PNS, they will have profound implications for the dynamics, nucleosynthesis, and neutrino signals of the supernova.

ACKNOWLEDGMENTS

We thank J. Martin and C. Yi for valuable discussions. This work is supported by the U.S. DOE EPSCoR Grant No. DE-SC0008142 and the NP Grant No. DE-SC0017803 at UNM for S. A. and H. D., “Gravitation et physique fondamentale” (GPHYS) of the Observatoire de Paris for S. A. and M. C. V., and JSPS and MEXT KAKENHI Grants (No. JP15K05093, No. JP17H01130, No. JP17K14306, No. 18H01212) and (No. JP26104006, No. 17H05206, No. JP17H06357, No. JP17H06364, No. JP17H06365) for K. S. and T. T., respectively. K. S. and T. T. acknowledge the support on the computing resources at NAOJ, KEK, Japan Lattime Data Grid (JLDG), YITP, Research Center for Nuclear Physics in Osaka University (RCNP), The University of Tokyo (UT) as well as Post-K and K-computer of the RIKEN AICS.

APPENDIX: THE OPTICAL DEPTHS

In this Appendix, we provide the information of the optical depths in the $t_{\mathrm{pb}} = 200$ ms snapshot of the 2D supernova model shown in Fig. 1. The optical depth of a neutrino is defined as

$$\tau(s) = \int_s^\infty \chi(s')\mathrm{d}s', \tag{A1}$$

where $\chi(s)$ is the neutrino opacity, and the integration is performed along the radial coordinate for the neutrinos in the forward angle bin. In the first three panels of Fig. 4, we show the optical depths of the neutrinos of different flavors and all with energy $E_\nu = 20.9$ MeV. The very right panel of the figure shows the matter density in this snapshot and the location of the neutrinospheres (where $\tau = 2/3$) for these neutrinos. The average energies of the neutrinos are in the range of 10–25 MeV in this snapshot.

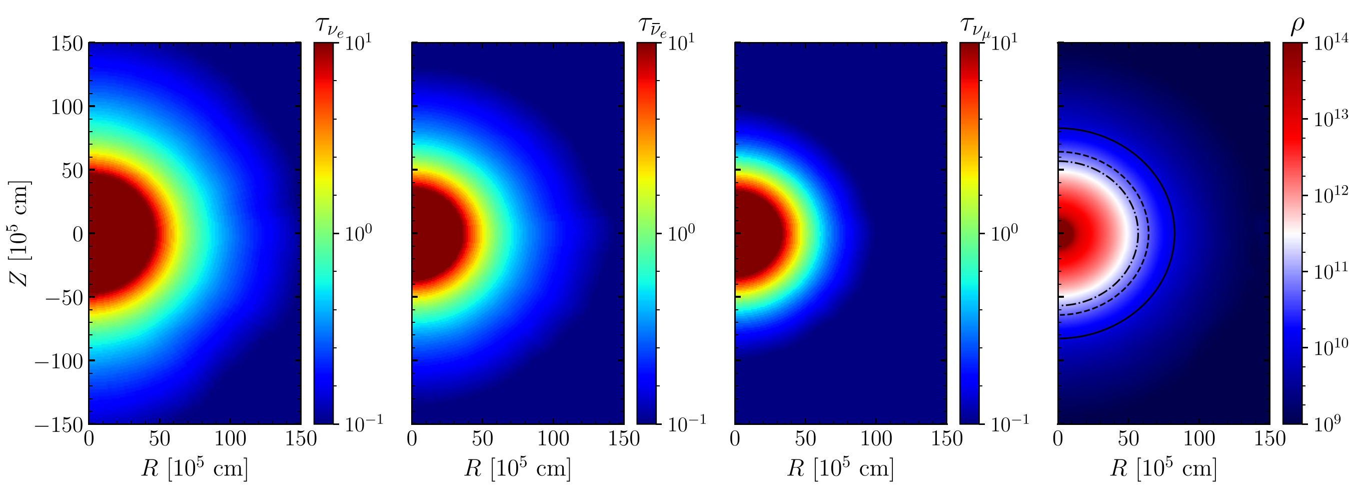

FIG. 4. The optical depths τ for the neutrinos of different flavors and with energy $E_\nu = 20.9$ MeV (the first three panels) and the matter density (the very right panel) in the $t_{\mathrm{pb}} = 200$ ms snapshot of the 2D supernova model shown in Fig. 1. The solid, dashed and dot-dashed circles in the right panel indicate the location of the neutrinospheres of these neutrinos.

[1] H. A. Bethe and J. R. Wilson, Revival of a stalled supernova shock by neutrino heating, Astrophys. J. **295**, 14 (1985).
[2] H.-T. Janka, Explosion mechanisms of core-collapse supernovae, Annu. Rev. Nucl. Part. Sci. **62**, 407 (2012).
[3] A. Burrows, Colloquium: Perspectives on core-collapse supernova theory, Rev. Mod. Phys. **85**, 245 (2013).
[4] Y. Z. Qian and S. E. Woosley, Nucleosynthesis in neutrino driven winds: 1. The physical conditions, Astrophys. J. **471**, 331 (1996).
[5] J. Gava, J. Kneller, C. Volpe, and G. C. McLaughlin, A Dynamical Collective Calculation of Supernova Neutrino Signals, Phys. Rev. Lett. **103**, 071101 (2009).
[6] S. Horiuchi, J. F. Beacom, and E. Dwek, The diffuse supernova neutrino background is detectable in Super-Kamiokande, Phys. Rev. D **79**, 083013 (2009).
[7] J. F. Beacom, The diffuse supernova neutrino background, Annu. Rev. Nucl. Part. Sci. **60**, 439 (2010).
[8] A. Mirizzi, I. Tamborra, H.-T. Janka, N. Saviano, K. Scholberg, R. Bollig, L. Hudepohl, and S. Chakraborty, Supernova neutrinos: Production, oscillations and detection, Riv. Nuovo Cimento **39**, 1 (2016).
[9] S. Horiuchi, K. Sumiyoshi, K. Nakamura, T. Fischer, A. Summa, T. Takiwaki, H.-T. Janka, and K. Kotake, Diffuse supernova neutrino background from extensive core-collapse simulations of 8–100 $M_{\odot}$ progenitors, Mon. Not. R. Astron. Soc. **475**, 1363 (2018).
[10] S. Pastor and G. Raffelt, Flavor Oscillations in the Supernova Hot Bubble Region: Nonlinear Effects of Neutrino Background, Phys. Rev. Lett. **89**, 191101 (2002).
[11] H. Duan, G. M. Fuller, J. Carlson, and Y.-Z. Qian, Simulation of coherent non-linear neutrino flavor transformation in the supernova environment. 1. Correlated neutrino trajectories, Phys. Rev. D **74**, 105014 (2006).
[12] H. Duan, G. M. Fuller, J. Carlson, and Y.-Z. Qian, Coherent Development of Neutrino Flavor in the Supernova Environment, Phys. Rev. Lett. **97**, 241101 (2006).
[13] H. Duan, G. M. Fuller, and Y.-Z. Qian, Collective neutrino oscillations, Annu. Rev. Nucl. Part. Sci. **60**, 569 (2010).
[14] S. Chakraborty, R. Hansen, I. Izaguirre, and G. Raffelt, Collective neutrino flavor conversion: Recent developments, Nucl. Phys. **B908**, 366 (2016).
[15] L. Wolfenstein, Neutrino oscillations in matter, Phys. Rev. D **17**, 2369 (1978).
[16] L. Wolfenstein, Neutrino oscillations and stellar collapse, Phys. Rev. D **20**, 2634 (1979).
[17] S. P. Mikheyev and A. Yu. Smirnov, Resonance amplification of oscillations in matter and spectroscopy of solar neutrinos, Sov. J. Nucl. Phys. **42**, 913 (1985).
[18] A. Esteban-Pretel, A. Mirizzi, S. Pastor, R. Tomàs, G. G. Raffelt, P. D. Serpico, and G. Sigl, Role of dense matter in collective supernova neutrino transformations, Phys. Rev. D **78**, 085012 (2008).
[19] S. Sarikas, G. G. Raffelt, L. Hudepohl, and H.-T. Janka, Suppression of Self-Induced Flavor Conversion in the Supernova Accretion Phase, Phys. Rev. Lett. **108**, 061101 (2012).
[20] S. Chakraborty, T. Fischer, A. Mirizzi, N. Saviano, and R. Tomas, No Collective Neutrino Flavor Conversions During the Supernova Accretion Phase, Phys. Rev. Lett. **107**, 151101 (2011).
[21] M. Zaizen, T. Yoshida, K. Sumiyoshi, and H. Umeda, Collective neutrino oscillations and detectabilities in failed supernovae, Phys. Rev. D **98**, 103020 (2018).
[22] H. Duan and A. Friedland, Self-Induced Suppression of Collective Neutrino Oscillations in a Supernova, Phys. Rev. Lett. **106**, 091101 (2011).
[23] H. Duan and S. Shalgar, Flavor instabilities in the neutrino line model, Phys. Lett. B **747**, 139 (2015).
[24] S. Chakraborty, R. S. Hansen, I. Izaguirre, and G. Raffelt, Self-induced flavor conversion of supernova neutrinos on small scales, J. Cosmol. Astropart. Phys. 01 (2016) 028.
[25] S. Abbar, H. Duan, and S. Shalgar, Flavor instabilities in the multiangle neutrino line model, Phys. Rev. D **92**, 065019 (2015).
[26] S. Abbar and H. Duan, Neutrino flavor instabilities in a time-dependent supernova model, Phys. Lett. B **751**, 43 (2015).
[27] B. Dasgupta and A. Mirizzi, Temporal instability enables neutrino flavor conversions deep inside supernovae, Phys. Rev. D **92**, 125030 (2015).
[28] R. F. Sawyer, Speed-up of neutrino transformations in a supernova environment, Phys. Rev. D **72**, 045003 (2005).
[29] R. F. Sawyer, Neutrino Cloud Instabilities Just Above the Neutrino Sphere of a Supernova, Phys. Rev. Lett. **116**, 081101 (2016).
[30] S. Chakraborty, R. Sloth Hansen, I. Izaguirre, and G. Raffelt, Self-induced neutrino flavor conversion without flavor mixing, J. Cosmol. Astropart. Phys. 03 (2016) 042.
[31] I. Izaguirre, G. Raffelt, and I. Tamborra, Fast Pairwise Conversion of Supernova Neutrinos: A Dispersion-Relation Approach, Phys. Rev. Lett. **118**, 021101 (2017).
[32] M.-R. Wu and I. Tamborra, Fast neutrino conversions: Ubiquitous in compact binary merger remnants, Phys. Rev. D **95**, 103007 (2017).
[33] F. Capozzi, B. Dasgupta, E. Lisi, A. Marrone, and A. Mirizzi, Fast flavor conversions of supernova neutrinos: Classifying instabilities via dispersion relations, Phys. Rev. D **96**, 043016 (2017).
[34] B. Dasgupta, A. Mirizzi, and M. Sen, Fast neutrino flavor conversions near the supernova core with realistic flavor-dependent angular distributions, J. Cosmol. Astropart. Phys. 02 (2017) 019.
[35] S. Abbar and H. Duan, Fast neutrino flavor conversion: Roles of dense matter and spectrum crossing, Phys. Rev. D **98**, 043014 (2018).
[36] S. Abbar and M. Cristina Volpe, On fast neutrino flavor conversion modes in the nonlinear regime, Phys. Lett. B **790**, 545 (2019).
[37] F. Capozzi, B. Dasgupta, A. Mirizzi, M. Sen, and G. Sigl, Collisional Triggering of Fast Flavor Conversions of Supernova Neutrinos, Phys. Rev. Lett. **122**, 091101 (2019).
[38] I. Tamborra, L. Huedepohl, G. Raffelt, and H.-T. Janka, Flavor-dependent neutrino angular distribution in core-collapse supernovae, Astrophys. J. **839**, 132 (2017).
[39] I. Tamborra, F. Hanke, H.-T. Janka, B. Müller, G. G. Raffelt, and A. Marek, Self-sustained asymmetry of lepton-number emission: A new phenomenon during the supernova shock-accretion phase in three dimensions, Astrophys. J. **792**, 96 (2014).

[40] K. Sumiyoshi and S. Yamada, Neutrino transfer in three dimensions for core-collapse supernovae. I. Static configurations, Astrophys. J. Suppl. Ser. **199**, 17 (2012).

[41] K. Sumiyoshi, T. Takiwaki, H. Matsufuru, and S. Yamada, Multi-dimensional features of neutrino transfer in core-collapse supernovae, Astrophys. J. Suppl. Ser. **216**, 5 (2015).

[42] H. Nagakura, W. Iwakami, S. Furusawa, H. Okawa, A. Harada, K. Sumiyoshi, S. Yamada, H. Matsufuru, and A. Imakura, Simulations of core-collapse supernovae in spatial axisymmetry with full Boltzmann neutrino transport, Astrophys. J. **854**, 136 (2018).

[43] G. Sigl and G. Raffelt, General kinetic description of relativistic mixed neutrinos, Nucl. Phys. **B406**, 423 (1993).

[44] A. Banerjee, A. Dighe, and G. Raffelt, Linearized flavor-stability analysis of dense neutrino streams, Phys. Rev. D **84**, 053013 (2011).

[45] P. Strack and A. Burrows, A generalized Boltzmann formalism for oscillating neutrinos, Phys. Rev. D **71**, 093004 (2005).

[46] C. Y. Cardall, Liouville equations for neutrino distribution matrices, Phys. Rev. D **78**, 085017 (2008).

[47] C. Volpe, D. Vnnen, and C. Espinoza, Extended evolution equations for neutrino propagation in astrophysical and cosmological environments, Phys. Rev. D **87**, 113010 (2013).

[48] A. Vlasenko, G. M. Fuller, and V. Cirigliano, Neutrino quantum kinetics, Phys. Rev. D **89**, 105004 (2014).

[49] G. M. Fuller, R. W. Mayle, J. R. Wilson, and D. N. Schramm, Resonant neutrino oscillations and stellar collapse, Astrophys. J. **322**, 795 (1987).

[50] D. Nötzold and G. Raffelt, Neutrono dispersion at finite temperature and density, Nucl. Phys. **B307**, 924 (1988).

[51] J. T. Pantaleone, Dirac neutrinos in dense matter, Phys. Rev. D **46**, 510 (1992).

[52] D. Vnnen and C. Volpe, Linearizing neutrino evolution equations including neutrino-antineutrino pairing correlations, Phys. Rev. D **88**, 065003 (2013).

[53] J. M. Lattimer and F. D. Swesty, A generalized equation of state for hot, dense matter, Nucl. Phys. **A535**, 331 (1991).

[54] T. Takiwaki, K. Kotake, and Y. Suwa, Three-dimensional hydrodynamic core-collapse supernova simulations for an 11.2 $M_{\odot}$ star with spectral neutrino transport, Astrophys. J. **749**, 98 (2012).

[55] T. Takiwaki, K. Kotake, and Y. Suwa, A comparison of two- and three-dimensional neutrino-hydrodynamics simulations of core-collapse supernovae, Astrophys. J. **786**, 83 (2014).

[56] D. Vartanyan, . Burrows, D. Radice, A. Skinner, and J. Dolence, A successful 3D core-collapse supernova explosion model, Mon. Not. R. Astron. Soc. **482**, 351 (2019).